Dawid BUŁA, Marian PASKO

Silesian University of Technology, Institute of Electrical Engineering and Computer Science

Dynamical properties of hybrid power filter with single tuned passive filter

Abstract. The paper has been intended to present the analysis of hybrid power filter (HPF) dynamical properties. The hybrid power filter with single tuned passive filter has been taken into consideration. The present paper deals with influence of control algorithm and its components on dynamical properties of HPF. Simulation and experimental results of transient states have also been included in the article.

*Streszczenie. W pracy zaprezentowano zagadnienia związane z właściwościami dynamicznymi hybrydowego energetycznego filtru aktywnego (HEFA) w konfiguracji z filtrem pasywnym jednej harmonicznej. Skupiono się na wpływie parametrów algorytmu sterowania na właściwości dynamiczne układu HEFA. Przedstawiono wyniki badań symulacyjnych oraz laboratoryjnych w stanach przejściowych pracy układu. (**Właściwości dynamiczne energetycznego filtru hybrydowego z filtrem pasywnym dla jednej harmonicznej**).*

Keywords: hybrid power filters, harmonics, transient states.
Słowa kluczowe: energetyczne filtry hybrydowe, harmoniczne, stany przejściowe.

Introduction

One of the methods to reduce harmonic distortion in power systems is using hybrid power filters [1, 2, 3, 4, 5]. Hybrid power filters combine two solutions i.e. active power filters with passive filters. Hybrid filters are usually used in medium voltage systems, where applying of pure active power filter is uneconomical and using passive filters is insufficient. There are also applications with hybrid filters in low voltage systems e.g. configurations with reduced passive filters and small rate active filters [6, 7, 8].

The development of power-electronic technology causes that characteristics of modern nonlinear loads have been changing. Fast variations of loads are the reason why dynamical properties of the used solution for harmonics filtration have become important. Both in active power filters and in hybrid filters dynamical properties in great measure depend on control strategy [1, 5] and its parameters.

The paper is a continuation of previous author's papers concerning hybrid power filter with single tuned passive filter [9, 10] and is focused on dynamical properties connected with control algorithm. Some of the presented dynamical problems, e.g. stability problem, are typical for hybrid filter and its feedback control.

Fig.1. System with the discussed hybrid power filter

Configuration of the system

Shunt hybrid power filter [2, 3, 5] usually consists of a passive filter tuned to the most often occurring higher harmonics (i.e. 5th, 7th, 11th). In the case considered the passive filter has been reduced to a single tuned filter [6, 7, 8, 9]. However, filtration of other (selected) harmonics

is possible by suitable modification of the control algorithm. Hybrid solution allows to decrease the active power filter power rating. On the other side reduction of passive part causes decrease of device weight and size.

Passive filter in this case is tuned to 7th harmonic frequency and is smaller and lighter than the filter tuned to the 5th-harmonic frequency. Moreover impedance of 7th harmonic filter for 5th harmonic as well for 11th harmonic frequency is still relatively low (fig. 2). It causes the small rate active part to be sufficient to compensate these harmonics.
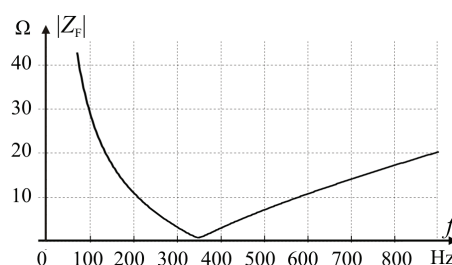

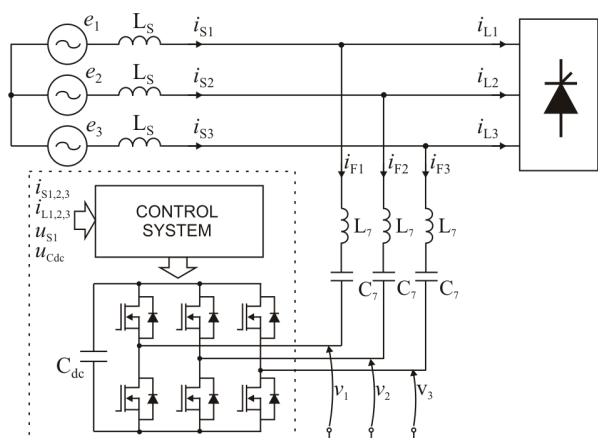Fig.2. The magnitude of impedance of 7th harmonic passive filter

Control principle

Active power filter voltage in shunt hybrid filter is usually proportional to higher harmonics of source current (i_{Sh}) [1, 2, 5]:

$$(1) \qquad V(j\omega) = K I_{Sh}(j\omega)$$

It causes improvement of attenuation characteristic in comparison to pure passive filter [2, 4]. The active power filter voltage for selected harmonics in this case is also dependent on harmonics of load current (i_{Lh}):

$$(2) \qquad V(j\omega) = K I_{Sh}(j\omega) + \sum_{n=5,11,13\ldots} {}_n K(j\omega) I_{Lh}(j\omega) Z_{Fn}$$

where: ${}_n K(j\omega)$ – frequency transfer function of filter for n-th harmonic, n – number of selected harmonics. Attenuation factor [2] in this case is given by:

$$(3) \qquad \gamma(j\omega) = \frac{I_{Sh}(j\omega)}{I_{Lh}(j\omega)} = \frac{Z_F(j\omega) - \sum\limits_{n=5,11,13\ldots} {}_n K(j\omega) Z_{Fn}}{Z_F(j\omega) + Z_S(j\omega) + K}$$

In the ideal case transfer function of filters for selected harmonics amounts one, whereas for other harmonics it is equal to zero. It produces the effect that numerator of (3) for particular harmonics equals zero.

Control strategy

Block diagram of control algorithm for reference voltages computation has been presented in fig. 3. The control algorithm is an implementation of control strategy given by (2) for three phase system. The presented algorithm can be divided into two parts – the upper with feedback control, which can realize fundamental algorithm, (1) and the lower with feedforward control, which is responsible for filtration of selected harmonics i.e. 5th, 11th and 13th in this case. Both parts use Clarke and Park transformations with suitable filters to determine the required components of source and load currents.
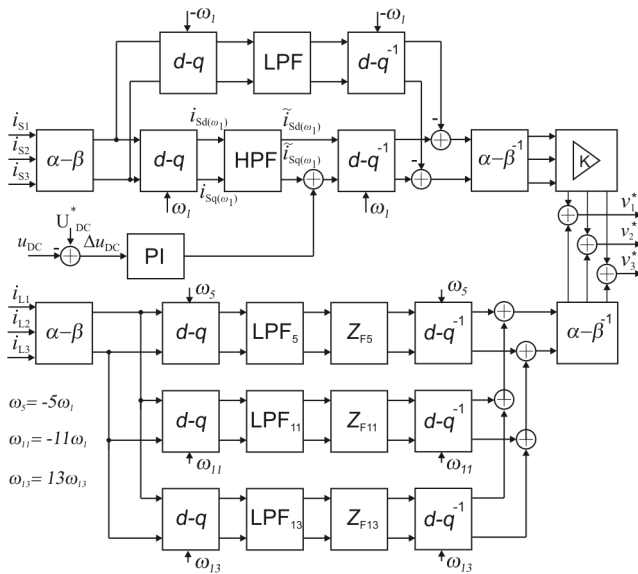

Fig.3. Diagram of the control system

Based on circuit from fig. 1 and diagram from fig. 3 frequency model for higher harmonics has been prepared (fig. 4). In the presented frequency model execution part (voltage converter) and DC-voltage controller have been omitted. By using the prepared model one can obtain:

$$
(4) \quad \begin{bmatrix} I_{S\alpha}(j\omega) \\ I_{S\beta}(j\omega) \end{bmatrix} = \left[Z_F(j\omega)\boldsymbol{I} + Z_s(j\omega)\boldsymbol{I} + K\big(\boldsymbol{G}_1(j\omega) - \boldsymbol{G}_{1N}(j\omega)\big) \right]^{-1}
$$

$$
\cdot \left[Z_F(j\omega)\boldsymbol{I} - \sum_n \boldsymbol{G}_2(j\omega)\boldsymbol{Z}_{Fn} \right] \begin{bmatrix} I_{L\alpha}(j\omega) \\ I_{L\beta}(j\omega) \end{bmatrix}
$$

where: $\boldsymbol{I}$ – 2 x 2 identity matrix, $Z_F(j\omega)$ – passive filter impedance, $Z_S(j\omega)$ – source impedance, K – hybrid filter gain, $\boldsymbol{G}_1(j\omega)$ – matrix connected with Park transformation and high pass filter (HPF) in feedback control [5, 11]:

$$
(4) \quad \boldsymbol{G}_1(j\omega) = \boldsymbol{D}(j\omega)^{-1} \boldsymbol{N}(j\omega)
$$

$$
(5\text{-}8) \quad \boldsymbol{D}(j\omega) = D(\lambda), \boldsymbol{N}(j\omega) = N(\lambda), \lambda = \begin{bmatrix} j\omega & \omega_1 \\ -\omega_1 & j\omega \end{bmatrix}
$$

$$
(9) \quad K_{HPF}(j\omega) = N(j\omega) / D(j\omega)
$$

$\boldsymbol{G}_{1N}(j\omega)$ – matrix corresponding with Park transformation and low pass filter (LPF) in feedback control (used for computation negative sequence of source currents):

$$
(10) \quad \boldsymbol{G}_{1N}(j\omega) = \boldsymbol{D}_N(j\omega)^{-1} \boldsymbol{N}_N(j\omega)
$$

$$
(11\text{-}12) \quad \boldsymbol{D}_N(j\omega) = D_N(\lambda_N), \boldsymbol{N}_N(j\omega) = N_N(\lambda_N)
$$

$$
(13) \quad \lambda_N = \begin{bmatrix} j\omega & -\omega_1 \\ \omega_1 & j\omega \end{bmatrix}
$$

$$
(14) \quad K_{LPF}(j\omega) = N_N(j\omega) / D_N(j\omega)
$$

$\boldsymbol{G}_{2,n}(j\omega)$ – matrixes connected with Park transformation and low pass filters (LPF$_n$) in feedforward control:

$$
(15) \quad \boldsymbol{G}_{2,n}(j\omega) = \boldsymbol{D}_n(j\omega)^{-1} \boldsymbol{N}_n(j\omega)
$$

$$
(16\text{-}17) \quad \boldsymbol{D}_n(j\omega) = D_n(\lambda_n), \boldsymbol{N}_n(j\omega) = N_n(\lambda_n)
$$

$$
(18) \quad \lambda_n = \begin{bmatrix} j\omega & \omega_n \\ -\omega_n & j\omega \end{bmatrix}
$$

$$
(19) \quad K_{LPFn}(j\omega) = N_n(j\omega) / D_n(j\omega)
$$

$$
(20\text{-}23) \quad n = 5,11,13, \quad \omega_5 = -5\omega_1, \quad \omega_{11} = -11\omega_1, \quad \omega_{13} = 13\omega_1
$$

$\boldsymbol{Z}_{Fn}$ – matrix connected with passive filter impedance for n-harmonic:

$$
(24) \quad \boldsymbol{Z}_{Fn} = \begin{bmatrix} \mathrm{Re}\{Z_F(j\omega_n)\} & \mathrm{Im}\{Z_F(j\omega_n)\} \\ -\mathrm{Im}\{Z_F(j\omega_n)\} & \mathrm{Re}\{Z_F(j\omega_n)\} \end{bmatrix}
$$

There is coupling between α on β components. Therefore it is not possible to obtain $I_{S\alpha}/I_{L\alpha}$ and $I_{S\beta}/I_{L\beta}$ filtering characteristics, but after transformation to positive/negative sequence according to:

$$
(25) \quad \begin{bmatrix} I_P \\ I_N \end{bmatrix} = \sqrt{\frac{1}{2}} \begin{bmatrix} 1 & j \\ 1 & -j \end{bmatrix} \begin{bmatrix} I_\alpha \\ I_\beta \end{bmatrix}
$$

it is possible to determine I_{SP}/I_{LP} and I_{SN}/I_{LN} filtering characteristics, which have been shown in fig. 5.
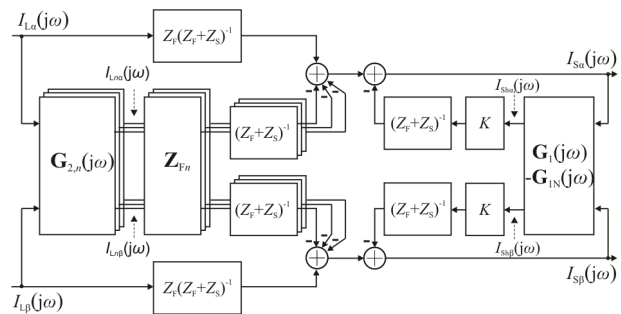

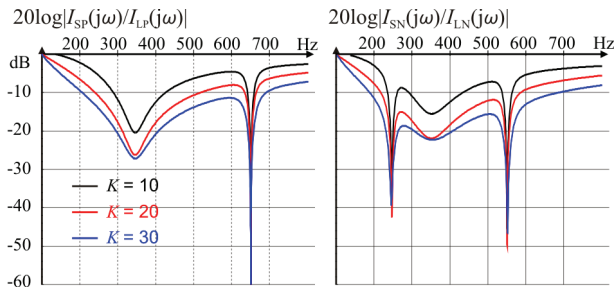Fig.4. Frequency model diagram of the discussed system

Fig.5. Filtering characteristics of the hybrid power filter for different hybrid filter gain

Signal filters

Signal filters used in control algorithm are elements with significant influence on dynamical properties of the whole hybrid power filter. On the one hand lower cut-off frequency of filters causes better filtration properties (fig. 6), on the other, it brings about extension of step response transient time. Example set of frequency and step responses for 2nd order Butterworth filters with different cut-off frequency has been shown in fig. 7. When frequency characteristic of filtered signals are known, filter parameters can been chosen. For low pass filter (LPF) 16 Hz cut-off frequency has been established. For other filters cut-off frequency has been set at 25 Hz. Second order Butterworth filters have been chosen in all cases.

It should be noticed that filters in feedback control (LPF, HPF) also have significant influence on stability of hybrid filters.
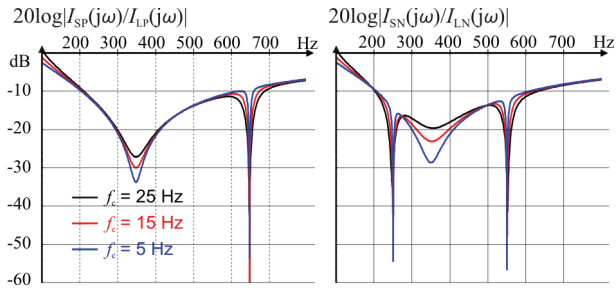

Fig.6. Filtering characteristics of the hybrid filter for different cut-off frequency of signal filters in control algorithm
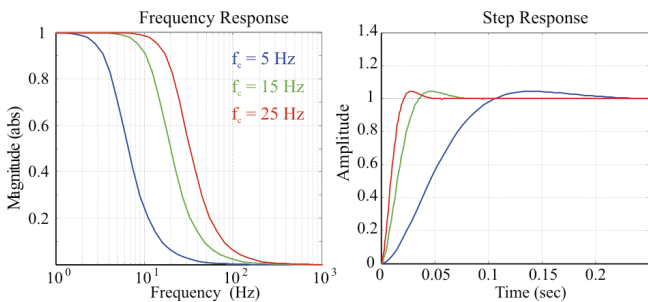

Fig.7. Frequency and step responses of 2nd order Butterworth filter

Stability analysis

Feedback control and delays in real control system [12] may cause stability problem. The diagram used for stability analysis has been presented in fig. 8a. Feedback transfer function in this case can be expressed as:

$$(26) \qquad H_{P,N}(j\omega) = \frac{KG_{P,N}(j\omega)e^{-j\omega\tau}}{Z_F(j\omega) + Z_S(j\omega)}$$

where $G_{P,N}(j\omega)$ is transfer function for positive and negative sequence is given by:

$$(27) \qquad \begin{bmatrix} G_P(j\omega) & 0 \\ 0 & G_N(j\omega) \end{bmatrix} = \\ = \frac{1}{2}\begin{bmatrix} 1 & j \\ 1 & -j \end{bmatrix}[G_1(j\omega) - G_{1N}(j\omega)]\begin{bmatrix} 1 & 1 \\ -j & j \end{bmatrix}$$

Hybrid power filter gain K and delay τ also have influence on stability of the system. Stability analysis has been made assuming that $\tau = 100$ μs [1, 12] and gain $K = 30$. Nyquist plots of feedback transfer function (25) for positive and negative sequence have been presented in figure 8b. Theoretical critical gain equaled 69 in this case.
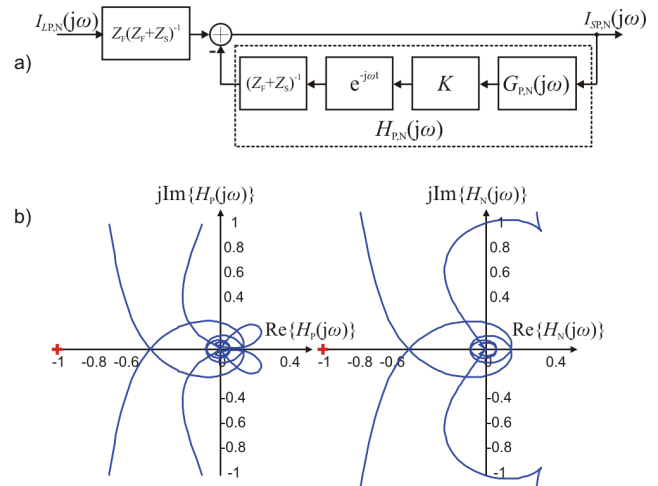

Fig.8. Stability analysis: a) block diagram used for the analysis b) Nyquist plots

DC-voltage control

Block diagram of the DC-voltage control is shown in fig. 9a. Example step responses for the DC-voltage control are also presented in fig. 9b. Parameters of PI controller can be calculated assuming T_I integral time and critically-damped response (damping ratio $\xi=1$ [8]) in which no voltage oscillation occurs in transient states. Based on these assumptions $T_I = 40$ ms and $K_P = 0.2$ have been assigned.
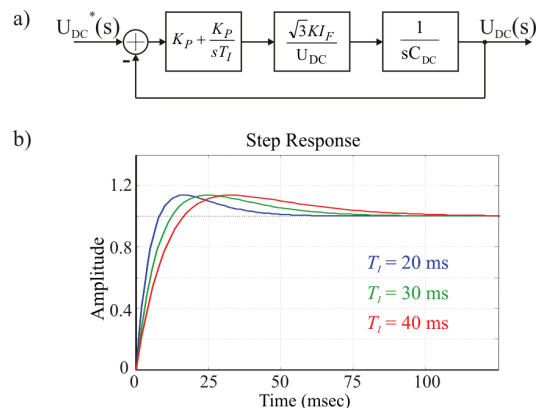

Fig.9. DC-voltage control: a) block diagram b) step responses

Simulation results

The discussed hybrid power filter has been simulated using SLPS interface (SimuLinkPSpice). SLPS makes it possible to carry out simulation of complex hardware-software systems simultaneously in two simulation

environments: Capture-PSpice and MATLAB-Simulink. Simulation tests have been made with the following parameters:

$|E_{1,2,3}|$ = 230 V, L_S = 0.5 mH, L_7 = 4.0 mH, C_7 = 52 μF, R_7 = 0.4 Ω, K = 30 Ω, U_{DC} = 60 V, C_{DC} = 4700 μF, f_{PWM} = 25 kHz.

The first test was made for balanced nonlinear load and consisted in step changing of load – from 3.5 kW to 5 kW. Simulation results have been presented in fig. 10. Transient state observable in source current waveforms lasts about 20 ms. It is clearly visible in fig. 11 where the selected control signals waveforms have been showed. Next test demonstrates the case with large delay in control, τ = 350 μs. Under these conditions the system loses stability which has been shown in waveforms in fig. 12. The last of the presented tests shows results (fig. 13) for step changing of unbalanced load.
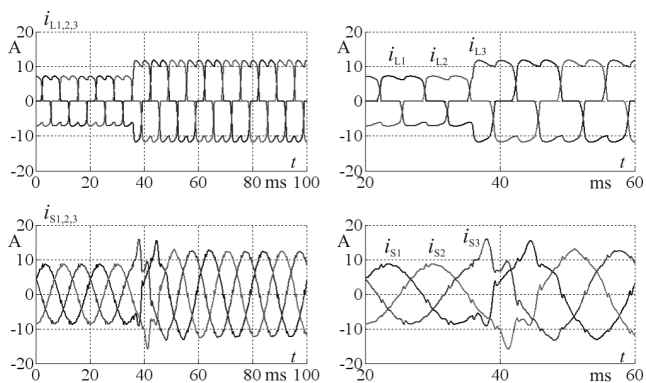

Fig.10. Simulation results for balanced load. Load currents $i_{L1,2,3}$ and source currents $i_{S1,2,3}$ waveforms
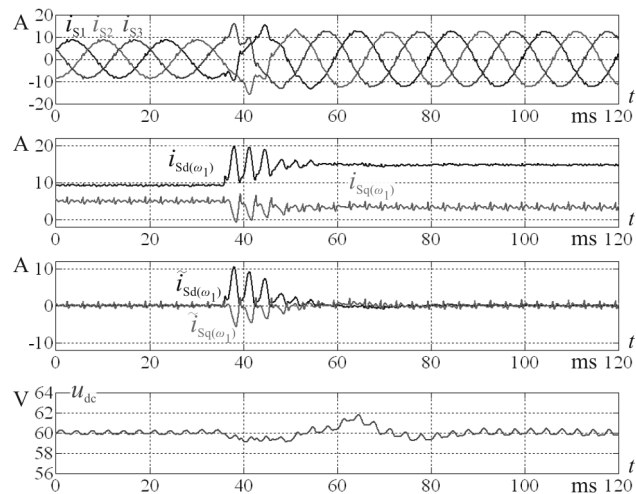

Fig.11 Simulation results for balanced load. Source currents $i_{S1,2,3}$, u_{dc} voltage and selected control signals waveforms
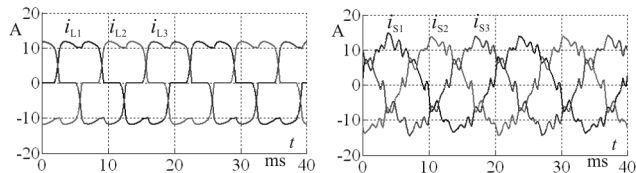

Fig.12 Simulation results for balanced load with large delay in control system. Load currents $i_{L1,2,3}$ and source currents $i_{S1,2,3}$ waveforms. Delay τ = 350 μs, K = 30
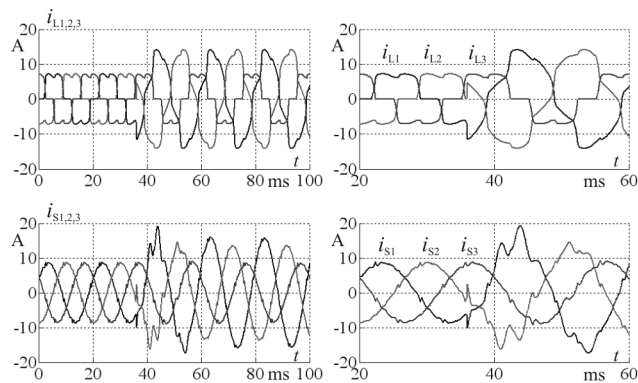

Fig.13. Simulation results for unbalanced load. Load currents $i_{L1,2,3}$ and source currents $i_{S1,2,3}$
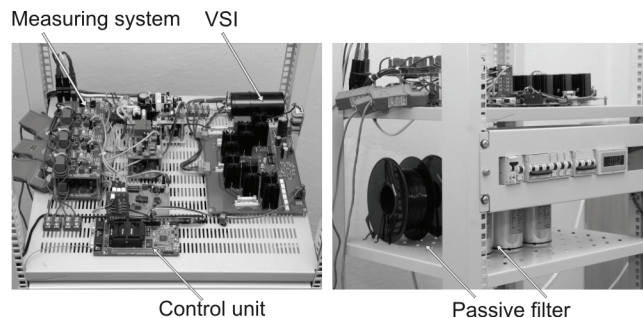

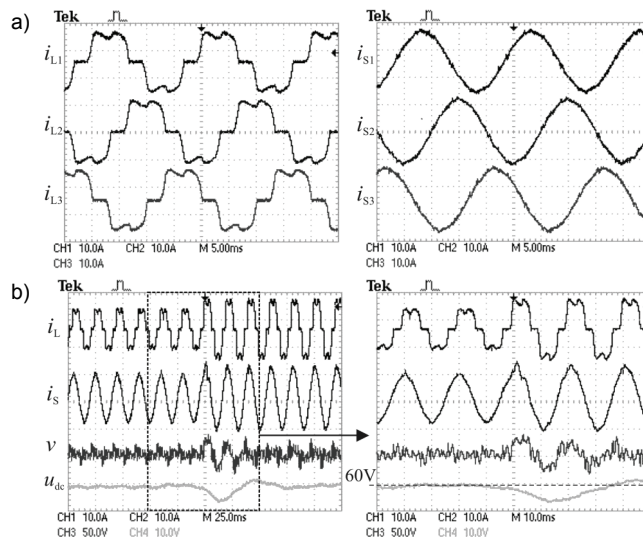Fig.14. Laboratory model of the hybrid power filter

Fig.15. Experimental results for balanced load: a) steady state, b) transient state

Experimental results

Experimental tests for the discussed hybrid power filter have been made with the same parameters as in simulation tests. Pictures of laboratory model, that was used in the experimental tests, have been presented in fig. 14. Experimental results of the two cases for dynamical properties verification have been presented in fig. 15 and fig. 16. The first test was made for balanced nonlinear load and consisted in step changing of load – from 3.5 kW to 5 kW. The second one consisted in connecting 2 kW unbalanced linear load to a 3.5 kW balanced nonlinear load. Experimental results for steady states after load change have also been shown in fig. 15 and 16. Total harmonic distortions of source currents after load change have been shown in tab. 1.

It can be noticed that the transient time in i_S source current waveforms was about 20 ms and in u_{DC} voltage

waveform was longer and equaled even 60 ms. Transient state in dc-voltage control was not visible in source currents waveforms.

Table 1. Total harmonic distortion before and after applying of hybrid power filter

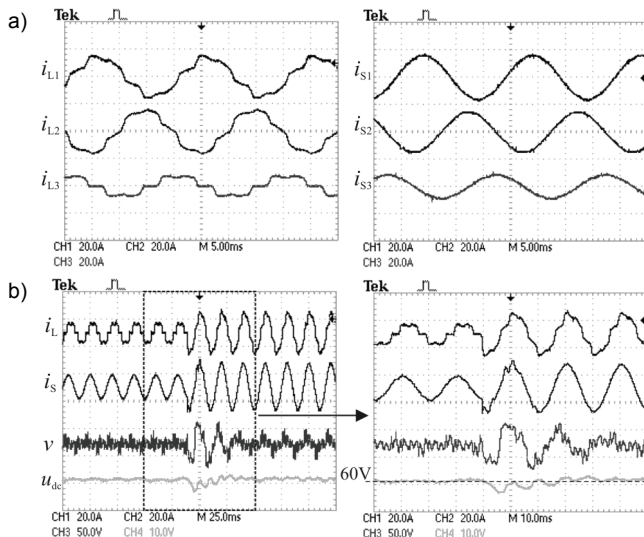|	Balanced load			Unbalanced Load		
	$THDi_{S1}$	$THDi_{S2}$	$THDi_{S3}$	$THDi_{S1}$	$THDi_{S2}$	$THDi_{S3}$
Before	24.8 %	24.6 %	24.7 %	14.0 %	12.4 %	25.3 %
After	3.4 %	3.3 %	3.3 %	2.1 %	2.4 %	3.5 %

Fig.16. Experimental results for unbalanced load: a) steady state, b) transient state

Summary

The present paper deals with influence of control algorithm and its components on dynamical properties of hybrid power filter with single tuned passive filter. For dynamical properties verification simulation and experimental results of transient states have been examined and included in the article.

While selecting control system parameters for the discussed hybrid filter it is necessary to compromise between excellent filtration and dynamical properties. However it is possible to obtain good characteristic of filtration and satisfactory dynamical properties, what has been proved in the article. Selection of control system parameters should be preceded by a stability analysis, because under certain conditions system can lose stability. One can draw the conclusion that the presented hybrid power filter can be used in systems with fast-variable loads.

REFERENCES
[1] H. Akagi, E. H. Watanabe, M. Aredes, Instantaneous Power Theory and Applications to Power Conditioning, *Wiley-IEEE Press*, Series Power Engineering, 2007
[2] S. Bhattacharya, P. Cheng, D. M. Divan, Hybrid Solution For Improving Passive Filter Performance In High Power Applications, *IEEE Trans. on Industry Applications*, vol. 33, no. 3, May/June 1997, 732-747
[3] M. Pasko, D. Buła, Hybrid Active Power Filters (in Polish), *Przegląd Elektrotechniczny*, no. 7/8, 2007, pp. 1-5.
[4] D. Rivas, L. Moran, J. W. Dixon, J. R. Espinoza, Improving passive filter compensation performance with active techniques, *IEEE Trans. on Industrial Electronics*, vol. 50, no. 1, 2003, 161-170
[5] R. Strzelecki, H. Supronowicz, Filtration of the harmonic in AC supply systems (in Polish), Toruń, Poland, *Adam Marszałek Publishing House*, 1997/1999
[6] H. Akagi, S. Srianthumrong, Y. Tamai, Comparisons in circuit configuration and filtering performance between hybrid and pure shunt active filters, *Conf. Rec. IEEE-IAS Ann. Meeting*, 2003, 1195-1202
[7] S. Srianthumrong, H. Akagi, A medium-voltage transformerless ac/dc power conversion system consisting of a diode rectifier and a shunt hybrid filter, *IEEE Trans. on Industry Applications*, vol. 39, no. 3, 2003, 874-882
[8] W. Tangtheerajaroonwong, T. Hatada, K. Wada, H Akagi, Design of a Transformerless Shunt Hybrid Filter Integrated into a Three-Phase Diode Rectifier, *Power Electronics Specialists Conference PESC '06*, 37th IEEE, 2006, 1-7
[9] Buła D., Pasko M.: Hybrid Active Power Filter with Single Tuned Passive Filter (in Polish), *Przegląd Elektrotechniczny*, no 12, 2009, 174-179
[10] Buła D., Pasko M.: Sensitivity Problem of Hybrid Active Power Filter with Single Tuned Passive Filter, *Przegląd Elektrotechniczny*, no 1, 2010, 59-61
[11] F. Z. Peng, H. Akagi, A. Nabae, Compensation Characteristics of the Combined System of Shunt Passive and Series Active Filters, *IEEE Trans. on Industry Applications*, vol. 29, no. 1, 1993, 144-152
[12] Buła D., Maciążek M., Pasko M., Optimization of time delays in Active Power Filter control algorithm, 8th International Workshop CPEE 2007, *Przegląd Elektrotechniczny – Konferencje*, no. 2, 2007, 102-105

Authors: *mgr inż. Dawid Buła, e-mail: dawid.bula@polsl.pl, prof. dr hab. inż. Marian Pasko, e-mail: marian.pasko@polsl.pl, Instytut Elektrotechniki i Informatyki, ul. Akademicka 10, 44-100 Gliwice*